

July 2008

XPS and Raman characterization of single-walled carbon nanotubes grown from pretreated Fe₂O₃ nanoparticles

Placidus B. Amama

Birck Nanotechnology Center, Purdue University, pamama@purdue.edu

Dmitry Zemlyanov

Birck Nanotechnology Center, Purdue University, dimazemlyanov@purdue.edu

B Sundarakannan

Department of Physics and Institute for Functional Materials, University of Puerto Rico

Ram S. Katiyar

School of Mechanical Engineering, Purdue University

Timothy Fisher

Birck Nanotechnology Center, Purdue University, tsfisher@purdue.edu

Follow this and additional works at: <http://docs.lib.purdue.edu/nanopub>

Amama, Placidus B.; Zemlyanov, Dmitry; Sundarakannan, B; Katiyar, Ram S.; and Fisher, Timothy, "XPS and Raman characterization of single-walled carbon nanotubes grown from pretreated Fe₂O₃ nanoparticles" (2008). *Birck and NCN Publications*. Paper 87.
<http://docs.lib.purdue.edu/nanopub/87>

This document has been made available through Purdue e-Pubs, a service of the Purdue University Libraries. Please contact epubs@purdue.edu for additional information.

XPS and Raman characterization of single-walled carbon nanotubes grown from pretreated Fe₂O₃ nanoparticles

Placidus B Amama^{1,4}, Dmitry Zemlyanov¹, B Sundarakannan²,
Ram S Katiyar² and Timothy S Fisher^{1,3,4}

¹ Birk Nanotechnology Center, Purdue University, West Lafayette, IN 47907, USA

² Department of Physics and Institute for Functional Materials, University of Puerto Rico, San Juan, PR 00931, USA

³ School of Mechanical Engineering, Purdue University, West Lafayette, IN 47907, USA

E-mail: pamama@purdue.edu and tsfisher@purdue.edu

Received 3 April 2008, in final form 22 May 2008

Published 31 July 2008

Online at stacks.iop.org/JPhysD/41/165306

Abstract

X-ray photoelectron (XPS) and Raman spectroscopic techniques have been used to study the influence of the annealing ambient (N₂, Ar and H₂) of nearly monodispersed Fe₂O₃ nanoparticles (mean size = 3.2 ± 1 nm) on the growth of carbon nanotubes by microwave plasma chemical vapour deposition. XPS characterization of the catalytic templates reveals that a N₂ ambient reduces sintering of the Fe₂O₃ nanoparticles and confirms that the chemical phase involved in the nucleation of nanotubes is the metal state Fe⁰. Multi-excitation wavelength Raman spectroscopy (514, 574, 633 and 785 nm) reveals that the single-walled carbon nanotubes (SWCNTs) grown from N₂-annealed catalyst nanoparticles range between 0.8 and 1.1 nm while SWCNTs grown from Ar-annealed catalyst nanoparticles exhibit a broader diameter distribution in the range 0.8–1.8 nm. The narrowness in the distribution of SWCNTs grown from the N₂-annealed catalysts has been attributed to the enhanced stability of Fe₂O₃ nanoparticles in an N₂ ambient.

(Some figures in this article are in colour only in the electronic version)

1. Introduction

To exploit the exceptional properties of single-walled carbon nanotubes (SWCNTs) in functional devices, a major obstacle that must be addressed is the ability to control the diameter and the atomic orientation of the nanoscale elements (chirality). Such control is highly critical for SWCNT assembly and integration because the electronic and optical properties depend strongly on these factors [1]. The growth of SWCNTs by microwave plasma chemical vapour depositions (MPCVDs) is highly challenging because the reactive plasma environment of the MPCVD makes it difficult to maintain a low carbon supply [2], an important precondition for SWCNT selectivity. In addition, catalyst nanoparticles having sizes within the range selective for SWCNT growth are typically unstable under thermal treatment, thereby rendering the use of

such nanoparticles as catalysts even more challenging. In the MPCVD growth environment, the possibility of catalyst coarsening and coalescence increases, resulting in catalyst deactivation and a decrease in SWCNT selectivity. Consequently, the use of MPCVD for carbon nanotube (CNT) growth has commonly focused on multi-walled carbon nanotubes (MWCNTs) [3] and carbon nanofibres [4]. Recently, SWCNTs have been successfully grown by MPCVD [5–10]; however, growth of high-quality SWCNTs of narrow diameter distribution and controlled chirality remains a major challenge.

In contrast to MPCVD, thermal CVD is presently well developed for SWCNT growth. A number of studies [11–16] have demonstrated reasonable control of the purity, wall selectivity, diameter, alignment and to some extent the chirality of SWCNTs grown via thermal CVD. Despite the progress in thermal CVD, the development of MPCVD growth techniques for controlling SWCNT properties remains crucial because for some applications SWCNT verticality is either advantageous

⁴ Author to whom any correspondence should be addressed.

or necessary, and MPCVD growth of CNTs allows for alignment in the direction of the electric field.

Earlier reports [5, 17] revealed the importance of the annealing ambient of the catalyst while the reactor temperature increases from room temperature to the synthesis temperature (900 °C). It was shown that annealing Fe₂O₃ nanoparticles in an N₂ ambient increases their stability [5]. The present work concentrates on the use of x-ray photoelectron (XPS) and multi-excitation Raman spectroscopy for elucidating the role of annealing ambient during nanotube growth in the MPCVD. XPS has provided insights into the chemical state of the catalysts, the sintering of the catalysts, the quality and the concentration (at%) of the carbon products. The results of resonance Raman scattering using excitation wavelengths of 514, 574, 633 and 785 nm reveal that annealing Fe₂O₃ nanoparticles in an N₂ ambient enhances diameter uniformity of SWCNTs. The Kataura plot has also been employed to predict the electronic properties of the SWCNTs synthesized from the N₂-annealed and Ar-annealed catalysts.

2. Experimental details

A fourth-generation, poly(amidoamine) (PAMAM) dendrimer terminated with an amine functional group (G4-NH₂) is used to deliver nearly monodispersed Fe₂O₃ nanoparticles to sapphire substrates. The dendrimer polymer: [NH₂(CH₂)₂NH₂](NH₂)₆₄, was supplied as a 10% CH₃OH solution from Aldrich. The catalyst solution was synthesized according to a recipe provided by Vohs *et al* [18]. A detailed description of the catalyst synthesis procedure has been reported [5]. Fe₂O₃ nanoparticles synthesized using a similar recipe was previously characterized by AFM (Veeco DI Dimension 3100) operating in the tapping mode. The process involved the measurement of the height profiles of individual nanoparticles [5]. The average size of the Fe₂O₃ nanoparticles was 3.2 ± 1 nm, and more than 90% of the nanoparticles were less than 5 nm in size, thus placing the catalyst in the size range selective for SWCNT growth [19]. With the dendrimer 'nanotemplate', it is possible to obtain monodispersed nanoparticles without severe aggregation on solid substrates [11]. The UV-Vis spectra of the Fe/G4-NH₂ solutions of different concentrations and pH (not shown for the sake of brevity) revealed the absence of the ligand-to-metal charge transfer (LMCT) transition occurring at 224 nm, which is considered evidence of the encapsulation of transition metal ions in the interior of the dendrimer matrix [20]. Therefore, *interdendritic* encapsulation, where multiple dendrimer molecules stabilize the surface of the Fe nanocomposite may account for the present templating mechanism.

The catalyst solution was prepared by mixing 0.12 mmol of the dendrimer and 1.89 mmol of FeCl₃ · 6H₂O for 4 h resulting in the formation of dendrimer-stabilized Fe(III) nanocomposites. The catalyst was immobilized on cleaned sapphire substrates by dip coating for 10 s, rinsing with deionized water to remove weakly bound nanocomposites and drying in N₂. The sapphire-supported dendrimer-stabilized catalyst was calcined at 550 °C for 5 min (heating rate = 30 °C min⁻¹) to remove the dendrimer, leaving a

monolayer of exposed nearly monodispersed Fe₂O₃. For the growth of SWCNTs by MPCVD, the calcined catalyst was placed on a 2 inch diameter Mo puck and introduced into the MPCVD reactor. The puck concentrates the plasma directly above the catalyst. The MPCVD chamber was evacuated to a pressure of 0.5 Torr using an external mechanical pump and then pressurized to 10 Torr using N₂. During the temperature ramp to 900 °C via induction substrate heating supplied by a 3.5 kW RF source acting on a graphite susceptor, different ambient gases (N₂, Ar or H₂) were introduced. Thereafter, 50 sccm H₂ gas was fed into the chamber to a final pressure of 10 Torr. The H₂ plasma was ignited using a power of 200 W, and 5 sccm of CH₄ was fed into the chamber for 20 min during which time nanotubes were synthesized. The chamber was evacuated and then allowed to cool to room temperature after each run.

The structural features of the as-synthesized nanotube samples grown from Fe₂O₃ nanoparticles annealed in the different ambient have been characterized comprehensively by FESEM and Raman spectroscopy, and are reported in [5]. H₂-annealed catalysts produced predominantly MWCNTs while N₂- and Ar-annealed catalysts produced predominantly SWCNTs. Multi-excitation wavelength Raman scattering spectroscopy was performed to assess the diameter distribution of SWCNTs grown from Fe₂O₃ nanoparticles annealed in N₂ and Ar. Excitation wavelengths of 514 (2.41 eV), 574 (2.16 eV), 633 (1.96 eV) and 785 nm (1.58 eV) were used. Each spectrum was an average of four independent spectra acquired from multiple spots on the sample. XPS was carried out using a Kratos Ultra DLD spectrometer equipped with a monochromatic Al K α radiation ($h\nu = 1486.58$ eV) and a commercial Kratos charge neutralizer. The survey spectra and high-resolution spectra were collected at fixed analyzer pass energies of 160 eV and 20 eV, respectively. The elemental composition in the near-surface region was calculated after the subtraction of a Shirley-type background and taking into account the corresponding Scofield atomic sensitivity factors and empirically chosen attenuation function to compensate the different attenuation lengths of photoelectrons emitted from the different electron levels with different kinetic energies. The binding energy (BE) values are referred to the Fermi level, and the energy scale was calibrated using the C 1s line at 284.8 eV. The XPS data were processed using the CasaXPS software [21].

3. Results and discussion

Figure 1 shows a summary of the effect of the annealing ambient of Fe₂O₃ nanoparticles on the quality of nanotubes and the amount of carbon (at%) produced. The quality of nanotubes has been estimated from the FWHM of the XPS C 1s peak and the ratio of the integrated intensity of the G-band relative to the D-band (I_G/I_D) in their Raman spectra, acquired with an excitation wavelength of 785 nm. The former quality index is not widely used. Won *et al* [22] have shown that the width of the XPS C1s peak correlates with improved crystallinity of the graphitic sheets. Both quality indexes show similar trend and indicate that N₂-annealed

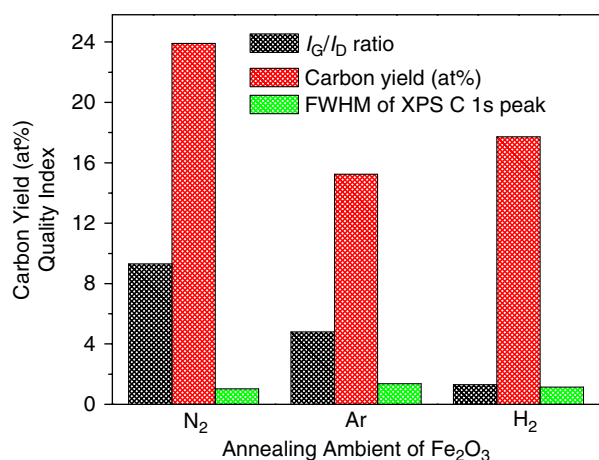


Figure 1. The effect of the annealing ambient of Fe₂O₃ nanoparticles on the carbon yield and the quality index of SWCNTs (I_G/I_D ratio and FWHM of XPS C 1s peak). The carbon yield and I_G/I_D ratio were obtained by XPS and Raman spectroscopy, respectively.

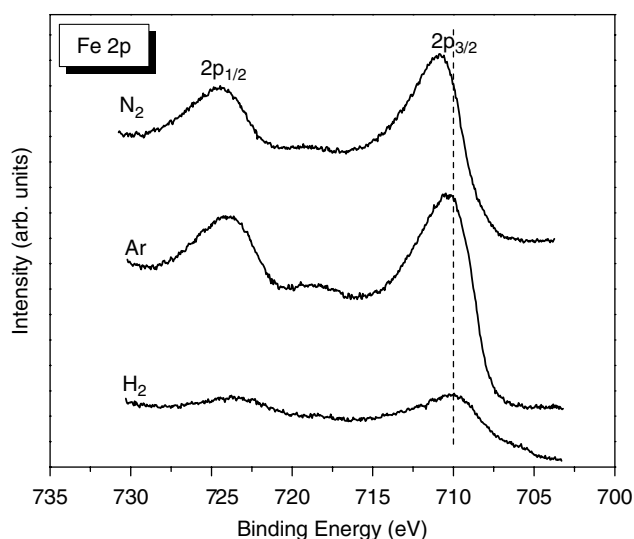


Figure 2. Calibrated XPS Fe 2p spectra for catalytic templates annealed in N₂, Ar and H₂ atmospheres without carbon deposition.

Fe₂O₃ nanoparticles produce nanotubes of the highest quality while H₂-annealed Fe₂O₃ nanoparticles produce nanotubes of the lowest quality. The amount of carbon produced from the different catalysts was determined by XPS, which represents carbon in the near-surface region of the sample. Nanotubes grown from N₂-annealed catalysts also showed the highest carbon amount (23.9 at%), followed by H₂-annealed catalysts with a carbon amount of 17.7 at%; the lowest carbon amount was observed for Ar-annealed catalysts (15.3 at%). Unlike H₂-annealed catalysts, the high carbon amount observed for catalysts annealed in N₂ is accompanied with a high I_G/I_D ratio suggesting that the carbon amount is not due to the formation of amorphous carbon but nanotubes or graphite.

XPS characterization of the catalytic templates was carried out after annealing in N₂, Ar and H₂ and their corresponding Fe 2p spectra are presented in figure 2. The Fe 2p peaks at 711 eV, 719 eV and 725 eV correspond to the binding energies of 2p_{3/2}, shake-up satellite 2p_{3/2} and 2p_{1/2}, respectively [23]; these peak

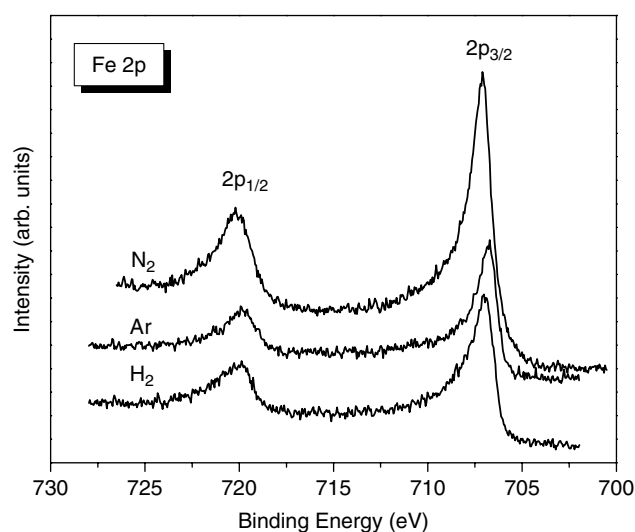
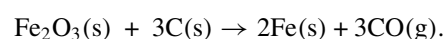


Figure 3. Calibrated XPS Fe 2p spectra for the catalytic templates annealed in N₂, Ar and H₂ atmospheres after carbon deposition.

positions are characteristic of Fe₂O₃. In our experiment, the 2p_{3/2} peaks for catalysts annealed in N₂, Ar and H₂ were centred at 710.8 eV, 710.3 eV and 709.9 eV, respectively. In addition, the 2p_{3/2} peak shoulders extends to lower energy regions as the annealing ambient is changed in the following order: N₂, Ar and H₂. These shoulders ~707 eV and ~710 eV correspond to binding energies for Fe and Fe₃O₄, respectively [24], and may account for the reduced stability observed in the case of H₂-annealed catalysts. Due to the inert nature of Ar, it is surprising that the Fe 2p_{3/2} peak shoulder for the Ar-annealed sample also extends to lower energy regions suggesting the presence of reduced Fe species. A possible explanation to this observation has been reported by Sohn *et al* [25] that during Ar pretreatment Fe₂O₃ can react with reactive carbon atoms to form reduced Fe as follows:



XPS characterization of the catalytic templates was carried out immediately after nanotube growth to determine the chemical state of the surface. Figure 3 shows the XPS Fe 2p spectra of the catalytic templates annealed in N₂, Ar and H₂ ambient after carbon deposition. The Fe 2p spectra are all characterized by two well-defined doublets at 720 and 707 eV (Fe 2p_{5/2}). The peak positions are typical for metallic iron [26]; this indicates that the active phase involved in the nucleation of CNTs in MPCVD under the present conditions is metal state Fe⁰ nanoparticles. This result is consistent with previous works [27] that have identified a reduced form of the transition metal particles as the active phase involved in the nucleation process.

A summary of the elemental compositions for catalysts annealed in N₂, Ar and H₂ after carbon deposition is shown in table 1. The amount of Fe (at%) on the substrate after carbon deposition as determined by XPS can explain the effect of the annealing ambient on Fe nanoparticles. The Fe concentration observed for catalysts annealed in N₂ ambient is 2.0 at%, which is approximately twice that observed for Ar- and H₂-annealed

Table 1. The elemental composition for catalysts annealed in N₂, Ar and H₂ after carbon deposition.

	Ambient	Al (at%)	C (at%)	Fe (at%)	O (at%)
N ₂		26.4	24.6	2.0	47.0
Ar		30.4	15.6	0.9	53.1
H ₂		30.0	18.2	1.2	50.6

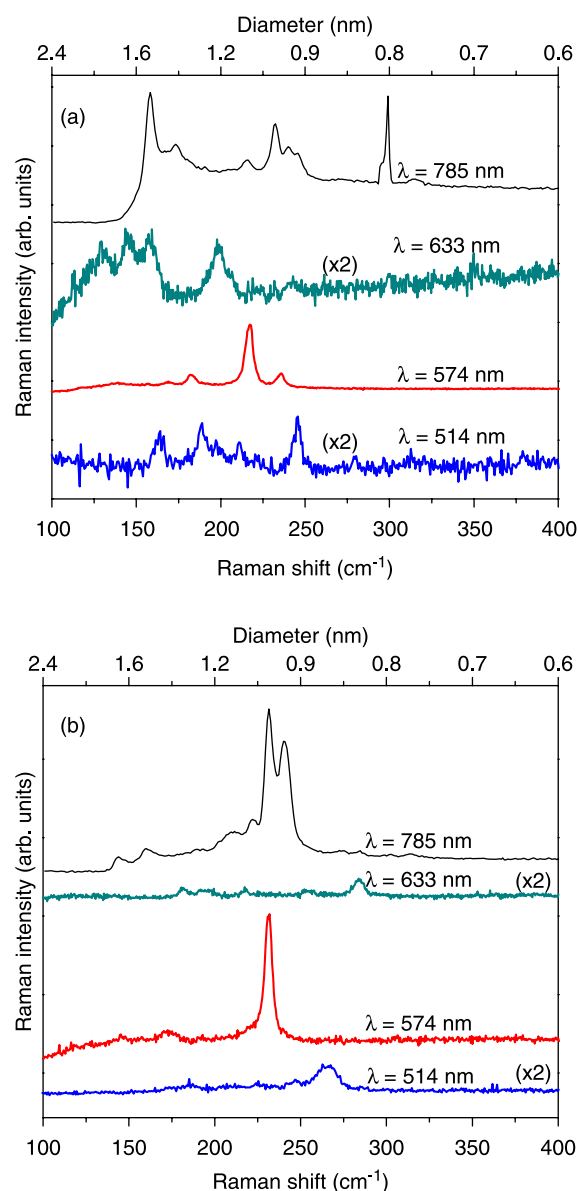
Fe₂O₃ nanoparticles. Because the initial Fe loading for all catalysts was the same, the difference in Fe amounts observed after growth may be related to its coverage on the substrate. Thus, if the Fe nanoparticles sinter, a lower Fe coverage (or dispersion) is expected; this is evidenced by the photoemission intensity of XPS Fe 2p spectra (figures 2 and 3), which is lowest for H₂-annealed catalysts. Annealing in an N₂ ambient seems to reduce the sintering of Fe nanoparticles and preserve the nanoparticles.

As presented in figure 1, the FWHMs of the C 1s band for SWCNT samples obtained from N₂-, Ar- and H₂-annealed catalysts were 1.03 eV, 1.36 eV and 1.14 eV, respectively. The low FWHM observed for SWCNTs grown from N₂-annealed catalysts is related to the increased crystalline perfection of the graphitic sheets and the presence of fewer defects. The quality results of CNTs obtained from both XPS and Raman spectroscopy (figure 1) are in consonance, and demonstrate the key role of N₂ during SWCNT growth by MPCVD.

The radial breathing mode (RBM) peaks of resonant Raman spectra of SWCNTs occurs in the low frequency region (100–400 cm⁻¹) and are considered as special signatures of SWCNTs. The intensity of the RBM peaks varies with the laser excitation energy because of the existence of a strong resonant enhancement effect, which emanates from the 1D quantum confinement of the electrons in the nanotube [28]. Therefore, for accurate characterization of the diameter distribution of SWCNTs, multi-excitation wavelength Raman spectroscopy is required to span several resonance conditions.

Figure 4 shows the Raman spectra of SWCNTs grown from Ar-annealed and N₂-annealed catalysts recorded at different excitation wavelengths (514, 574, 633 and 785 nm). The empirical relation $\omega_{\text{RBM}}(\text{cm}^{-1}) = 12.5 + 223.5/d_t(\text{nm})$, where ω_{RBM} is the frequency of the RBM peak and d_t is SWCNT diameter, was used to estimate the tube diameter [29]. SWCNTs grown from Ar-annealed Fe₂O₃ nanoparticles exhibit several RBM peaks in the range 130–299 cm⁻¹, which correspond to tube diameters in the range 0.8–1.8 nm (figure 4(a)). On the other hand, fewer RBM peaks, mainly in the range 231–284 cm⁻¹ were obtained for SWCNTs grown from N₂-annealed Fe₂O₃ nanoparticles, and they correspond to tube diameters in the range 0.8–1.0 nm (figure 4(b)). It is evident from this result that SWCNTs grown from N₂-annealed catalysts have a narrower diameter distribution than SWCNTs grown from Ar-annealed catalysts. The diameter range of SWCNTs grown from N₂-annealed catalysts is comparable to that reported for SWCNTs grown by the HiPCO process, which is between 0.7 and 1.1 nm [30].

The narrow diameter distribution observed for SWCNTs grown from N₂-annealed catalysts is attributable to the high stability of Fe₂O₃ nanoparticles in an N₂ ambient on the basis of Ostwald ripening [5]. The Fe–N species that may be formed

**Figure 4.** Raman spectra recorded at different excitation wavelengths showing the RBM regions for (a) SWCNTs grown from Ar-annealed Fe₂O₃ nanoparticles and (b) N₂-annealed Fe₂O₃ nanoparticles.

when Fe₂O₃ nanoparticles are annealed in N₂ would have a melting point well above that of pure Fe and would favour the stabilization of Fe₂O₃ nanoparticles. For nanotube growth by CVD, it has been widely reported [31] that the size of the catalyst nanoparticles correlates closely with the nanotube diameter. Therefore, by decreasing sintering or increasing the stabilization of Fe₂O₃ nanoparticles in an N₂ ambient, SWCNT selectivity and diameter uniformity are enhanced.

An attempt has been made to predict metallic and semiconducting behaviour of the SWCNTs grown through the use of a revised Kataura plot that is based on experimental data [32]. The plot correlates the $\omega_{\text{RBM}}(\text{cm}^{-1})$ to the resonant transition energies E_{ii} in the DOS for each SWCNT chirality (n, m). From the four excitation energies ($E = 1.58, 1.96, 2.16$ and 2.41 eV) employed for multi-excitation Raman spectroscopy and their corresponding d_t (or RBM

peak positions), the electronic character of SWCNTs can be predicted from the Kataura plot.

The analysis indicates the existence of both semiconducting (*s*-SWCNTs) and metallic (*m*-SWCNTs) SWCNTs for samples obtained from Fe₂O₃ nanoparticles annealed in Ar and N₂ ambient. Selective synthesis of only *s*-SWCNTs or *m*-SWCNTs is a major challenge that is currently being studied. We have previously shown that through the application of an applied substrate bias greater than -150 V, *m*-SWCNTs are selectively removed, leaving predominantly *s*-SWCNTs [33]. The drawback of this approach however is that SWCNT quality and density decrease significantly, in part, because of the bombardment of positively charged hydrogen and hydrocarbon ions generated in the plasma. It should be noted that the excitation at 633 nm (1.96 eV) is known to bring into resonance both *m*-SWCNTs and *s*-SWCNTs. Interestingly, predictions carried out on the basis of this excitation energy (1.96 eV) suggest that SWCNTs grown from N₂-annealed catalysts are mainly *s*-SWCNTs while SWCNTs grown from Ar-annealed catalysts are mixtures of *m*-SWCNTs and *s*-SWCNTs. This result may suggest the favoured production of *s*-SWCNTs for samples grown from N₂-annealed catalysts.

4. Conclusions

The influence of the annealing ambient of Fe₂O₃ nanoparticles on nanotube quality and amount, catalytic properties and the diameter distributions of SWCNTs produced by MPCVD has been elucidated. The results reveal the key role of the annealing ambient of catalyst nanoparticles in the highly reactive MPCVD growth environment. The use of multi-excitation Raman spectroscopy demonstrates that SWCNTs grown from N₂-annealed catalysts are of narrower diameter distribution (0.8–1.1 nm) in comparison with SWCNTs grown from Ar-annealed catalysts (0.8–1.8 nm). Characterization of the catalytic templates by XPS reveals that N₂ ambient reduces sintering of the Fe₂O₃ nanoparticles and enhances nanotube selectivity, amount and quality. Also, the active phase involved in the nucleation of nanotubes may be metal state Fe⁰ nanoparticles. The MPCVD growth technique offers several advantages and the results of this work would advance the use of Fe₂O₃ nanoparticles for controlled SWCNT growth by MPCVD.

Acknowledgments

This work is supported by the Purdue–NASA Institute for Nanoelectronics and Computing and the Birck Nanotechnology Center, Purdue University. The authors are grateful to Professor Lynne Taylor for access to the 785 nm excitation Raman system.

References

- [1] Saito R, Dresselhaus G and Dresselhaus M S 1998 *Physical Properties of Carbon Nanotubes* (London: Imperial College Press)
- [2] Delzeit L, Nguyen C V, Stevens R M, Han J and Meyyappan M 2002 *Nanotechnology* **13** 280
- [3] Meyyappan M, Delzeit L, Cassell A and Hash D 2003 *Plasma Sources Sci. Technol.* **12** 205
- [4] Melechko A V, Merkulov V I, McKnight T E, Guillorn M A, Klein K L, Lowndes D H and Simpson M L 2005 *J. Appl. Phys.* **97** 041301
- [5] Amama P B, Maschmann M R, Fisher T S and Sands T D 2006 *J. Phys. Chem. B* **110** 10636
- [6] Maschmann M R, Amama P B, Goyal A, Iqbal Z, Gat R and Fisher T S 2006 *Carbon* **44** 10
- [7] Li Y et al 2004 *Nano Lett.* **4** 317
- [8] Min Y-S, Bae E J, Oh B S, Kang D and Park W 2005 *J. Am. Chem. Soc.* **127** 12498
- [9] Zhang G et al 2005 *Proc. Natl Acad. Sci. USA* **102** 16141
- [10] Kato T, Jeong G-H, Hirata T, Hatakeyama R and Tohji K 2004 *Japan. J. Appl. Phys.* **43** L1278
- [11] Choi, H C, Kim W, Wang D and Dai H 2002 *J. Phys. Chem. B* **106** 12361
- [12] Bachilo S M, Balzano L, Herrera J E, Pompeo F, Resasco D E and Weisman R B 2003 *J. Am. Chem. Soc.* **125** 11186
Lolli G, Zhang L, Balzano L, Sakulchaicharoen N, Tan Y and Resasco D E 2006 *J. Phys. Chem. B* **110** 2108
- [13] Ciuparu D, Chen Y, Lim S, Haller G L and Pfefferle L 2004 *J. Phys. Chem. B* **108** 503
- [14] Yao Z, Kane C L and Dekker C 2000 *Phys. Rev. Lett.* **84** 2941
- [15] Ago H, Imamura S, Okazaki T, Saito T, Yumura M and Tsuji M 2005 *J. Phys. Chem. B* **109** 10035
- [16] Dai H 2002 *Acc. Chem. Res.* **35** 1035
- [17] Amama P B, Ogebule O, Maschmann M R, Sands T D and Fisher T S 2006 *Chem. Commun.* **27** 2899
- [18] Vohs J K, Brege J J, Raymond J E, Brown A E, Williams G L and Fahlman B D 2004 *J. Am. Chem. Soc.* **126** 9936
- [19] Li Y, Kim W, Zhang Y, Rolandi M, Wang D and Dai H 2001 *J. Phys. Chem. B* **105** 11424
Li Y, Liu J, Wang Y and Wang Z L 2001 *Chem. Mater.* **13** 1008
- [20] Scott R W J, Wilson O M and Crooks R M 2005 *J. Phys. Chem. B* **109** 692
- [21] Fairley N 1999–2006 CasaXPS version 2.3.12
- [22] Yoon S W, Kim S Y, Park J, Park C J and Lee C J 2005 *J. Phys. Chem. B* **109** 20403
- [23] Li X-q and Zhang W-x 2006 *Langmuir* **22** 4638
- [24] Mills P and Sullivan J L 1983 *J. Phys. D: Appl. Phys.* **16** 723
- [25] Sohn J I, Choi C-J, Seonghoon L and Seong T-Y 2001 *Appl. Phys. Lett.* **78** 3130
- [26] Kónya Z, Kiss J, Oszkó A, Siska A and Kiricsi I 2001 *Phys. Chem. Chem. Phys.* **3** 155
- [27] Herrera J E and Resasco D E 2003 *J. Phys. Chem. B* **107** 3738
Amama P B, Lim S, Ciuparu D, Yang Y, Pfefferle L and Haller G L 2005 *J. Phys. Chem. B* **109** 2645
- [28] Dresselhaus M S and Eklund P C 2000 *Adv. Phys.* **49** 705
- [29] Bachilo S M, Strano M S, Kittrell C, Hauge R H, Smalley R E and Weisman R B 2002 *Science* **298** 2361
- [30] O'Connell M J et al 2002 *Science* **297** 593
- [31] Cheung C L, Kurtz A, Park H and Lieber C M 2002 *J. Phys. Chem. B* **106** 2429
Ciuparu D, Chen Y, Lim S, Haller G L and Pfefferle L 2004 *J. Phys. Chem. B* **108** 503
- [32] Dresselhaus M S, Dresselhaus G and Jorio A 2007 *J. Phys. Chem. C* **111** 17887
- [33] Maschmann M R, Amama P B, Goyal A, Iqbal Z and Fisher T S 2006 *Carbon* **44** 2758